

SMASIS2013-3269

EFFECTS OF ALTITUDE ON ACTIVE STRUCTURAL HEALTH MONITORING

Benjamin Cooper
Department of Mechanical Engineering, Graduate Studies, New Mexico Tech,
Socorro, New Mexico, USA

Andrei Zagrai

Seth Kessler
Metis Design Corporation, Boston, MA, USA

ABSTRACT

As the field of Structural Health Monitoring (SHM) expands to spacecraft applications, the understanding of environmental effects on various SHM techniques becomes paramount. In January of 2013, an SHM payload produced by New Mexico Tech was sent on a high altitude balloon flight to a full altitude of 102,000 ft. The payload contained various SHM experiments including impedance measurements, passive detection (acoustic emission), active interrogation (guided waves), and wireless strain/temperature sensing. The focus of this paper is the effect of altitude on the active SHM experiments. The active experiment utilized a commercial SHM product for generation and reception of elastic waves that enabled wavespeed measurements, loose bolt detection, and crack detection through the full profile of the flight. Definite deviations were observed in the data through the stages of the flight which included a ground, ascent, float, and descent phases. Several elements of the high altitude environment can have an effect on the measurement such as temperature and pressure. The flight data was compared against a ground altitude baseline and heavy emphasis is placed on comparing changes in the data with the temperature profile of the flight. Conclusions are drawn on the effect of altitude on wavespeed of elastic waves, crack detection, and the sensing of a loose bolt.

INTRODUCTION

In the past, the New Mexico Institute of Mining and Technology has designed and flown an SHM payload for the purpose of exploring health monitoring sensors and techniques for space applications [1]. This payload focused on impedance type measurements to look for changes in structural dynamics during a sub-orbital rocket launch. The next iteration of the payload included several more experiments, one of which focused on guided waves [2]. Guided waves are a current favorite for SHM applications due to their long range capabilities to detect damage and structural changes in many

platforms including aerospace vehicles. SHM techniques have been identified as an important next step for enabling rapid satellite development and deployment. Within that scope, the use of guided waves to identify loose bolts and components has been expressed as an area of need [3]. This payload and its experiments seek to address some of these needs, but with the additional aim of understanding environmental factors. Temperature has been identified as an important element to consider for SHM aerospace applications and an investigation into its effect on Lamb waves (a special set of guided waves applicable to thin plate structures) has been undertaken by Dodson and Inman [4]. Several laboratory tests have been carried out to obtain temperature dependent data and develop strategies to compensate in the SHM techniques [5][6]. The contribution of this paper is to add to the investigation of environmental factors on the use of SHM techniques for space and high altitude application. Sending the payload on a high altitude balloon allows the collection of data in a full high altitude environment which may include extra influences not replicated in laboratory tests. Because temperature is such a strong factor, the first step is to link the temperature profile of the flight with the data collected using guided waves. A temperature profile and elevation of the payload is presented in Figure 1. After understanding the temperature influence on the data, any discrepancies can be explored and attributed to other factors, such as pressure.

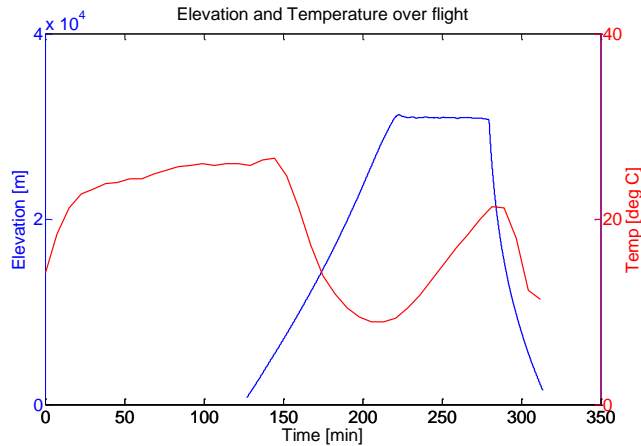


Figure 1 Overlay of temperature and elevation of the payload throughout the duration of the flight.

EXPERIMENTAL SETUP

Although the full payload included several experiments, only the relevant portions to the active SHM will be described. The payload is constructed of several circular plates and long thin rods. Each tier of the payload has one or more functions. The guided wave plates were kept as unobstructed as possible to allow for clean signals to be captured. Two plates and 7 piezoelectric sensors were used in the guided wave experiment. A single sensor (labeled as S0(A) in Figure 2) served solely as an actuator. All other sensors (S1 through S6) were only receivers creating an entirely pitch-catch type system. As a note, the haphazard placement of sensor labels is a product of the labels the collection hardware specifies and minimizing the wire routing for each sensor. Elastic waves are generated at frequencies from 50kHz to 500kHz in 25kHz step and the data is organized into three experimental goals.

(1) Wavespeed/Phase shift: Several of the sensors have unobstructed paths from the actuator (S0). This allows for calculation of the wave speeds of the pulses given the known distance and time of arrival.

(2) Loose bolt detection: The plates of the payload are connected by a threaded rod and bolts that clamp the plates together. All of the rods and bolts are properly tightened, except for one which is looser than the rest (highlighted in red). Sensors S3 and S4 are located at the bottom of the transmission path through the threaded rod pillars to pick up the transmitted pulse, one through a healthy pillar and one through the “damaged” loose bolt pillar.

(3) Crack detection: A simulated crack was cut in the top experiment plate. There are sensors (S5 and S1) to receive the guided wave passing through the crack (through transmission), and to receive the reflected wave from the crack respectively.

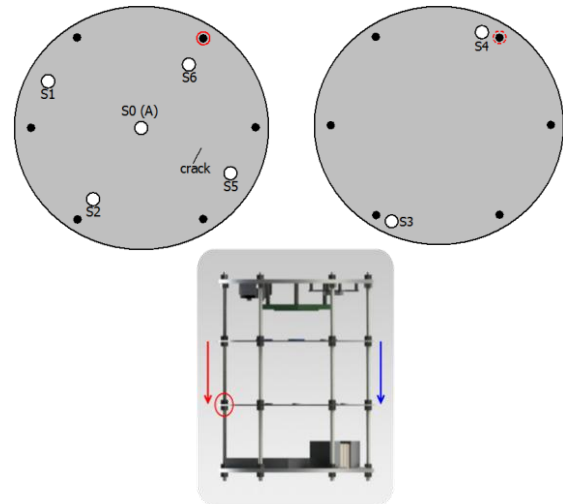


Figure 2 (Top) Plates with sensors for crack detection (S1/S5), loose bolt detection (S3/S4), and free path wave speed measurement (S2/S6) (Bottom) Illustration of damaged vs. healthy pillar with highlighted loose bolt

FLIGHT RESULTS

Wavespeed Phase Shifts

The earliest observation that came out of the data was the shift in the waveform throughout the flight as seen in Figure 3. The Ground stage can be thought of as a baseline, therefore the Ascent, Float, and Descent waveforms are all deviations from the ground baseline. In general, the shift increases with altitude which would tend to follow the trend of temperature decreasing with altitude. However, there is that area at the float altitude that warms up slightly which will be seen later in both temperature and phase shift plots. This high altitude warming trend is mentioned in the Near Space “Payload User’s Guide” and data on expected temperatures can be found from the National Oceanographic and Atmospheric Administration [7]. The Float waveform seen here is taken a little before the balloon reaches the max altitude and is therefore at its coldest point. A later Float data point will show a smaller shift. The Ascent and Descent waveforms follow logically since it is expected that similar levels of altitude (and likely temperature) will lead to similar shifts.

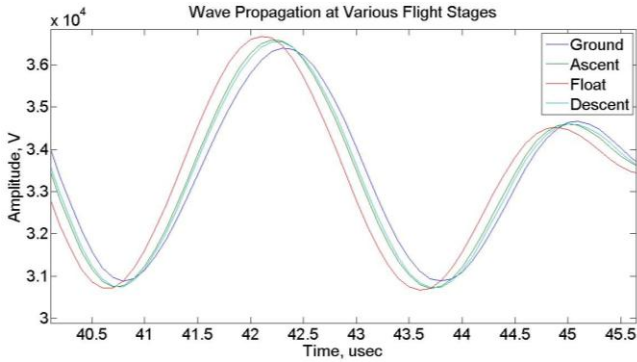


Figure 3 Demonstration of phase shift at various flight stages.

The data collection period started about 2 hours before the balloon lifted off, and the flight lasted around 3 hours. During these two periods about 42 full frequency sweeps were collected as well as temperature readings from an embedded sensor. Though the temperature sensor in the electronics won't give the exact environmental condition, it does track the relative change in temperature very well and allows us to compare waveform data with temperature data during the collection period. Figure 4 plots the phase shift from the initial ground condition as well as temperature over the course of the data collection. For the first 150 minutes the payload was sitting on the ground as the launch team performed various pre-flight checks and waited for good launch weather. The system was activated at 9am and sat outside during testing. There is a steady rise in temperature as first the electronics warm up (first 5-10 minutes), but then as the sun rises and payload and its container warm up. The container and payload are almost entirely metal and warm up an appreciable amount. There is a roughly equivalent phase shift in the waveforms as the temperatures rises. The payload is launched somewhere around the 120 minute mark and rises for the next 2 hours. The temperature drop is strongly present in the data. The phase shift swings strongly to the negative although with a slower rate. This could be due to the greater amount of material in the plate and the slower heat transfer away from it as a result. The temperature drops until the payload hits the float altitude (about 200 minutes in) where the temperature begins to rise again. Between 80,000 and 100,000 ft the atmospheric temperature may rise about 10°C. Indeed, the temperature gained back in the plot is a little over 10 degrees by the time the payload is instructed to terminate the balloon. At this point the payload dropped, deployed a parachute and descended through the coldest layers once again. The temperature drop before landing can also be seen as the final portion of data in Figure 4.

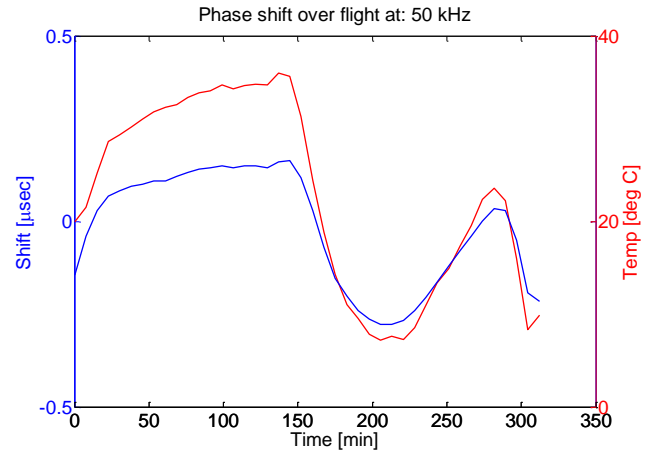


Figure 4 Phase shift and internal temperature over pre-flight and flight time for the 50kHz excitation.

Data was collected for 19 frequencies, but let's jump to the 200kHz phase shift and start discussing some patterns. It is already clear that the general pattern of the phase shifts follows the profile of the temperature of the flight. This supports the idea that temperature is the dominating factor for any environmental influence due to altitude. Jumping from 50 to 200kHz (see Figure 5), the two data sets seem to match each other more closely (scaled of course). Looking ahead to Figure 6 and Figure 7, the scaled profiles began to match each other more and more with increasing excitation frequency.

A thorough look into the papers relating wave propagation speed and temperature would help determine if the higher frequencies should follow the temperature more responsively or if this is an area that can be further explored with additional lab tests and/or future flights.

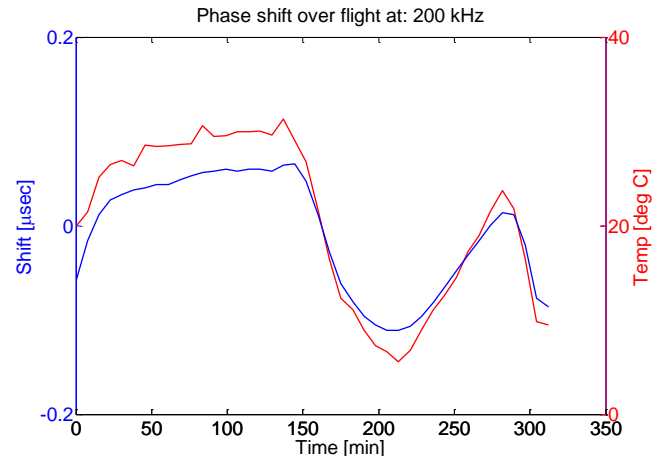


Figure 5 Phase shift and internal temperature for the 200kHz excitation. Note the closer aligning of the data shapes to each other

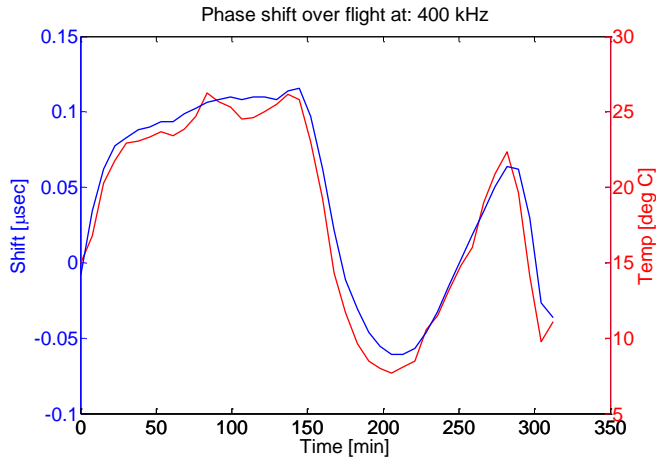


Figure 6 Phase shift and temperature for 400kHz excitation. Closest matching of phase shift and temp profiles

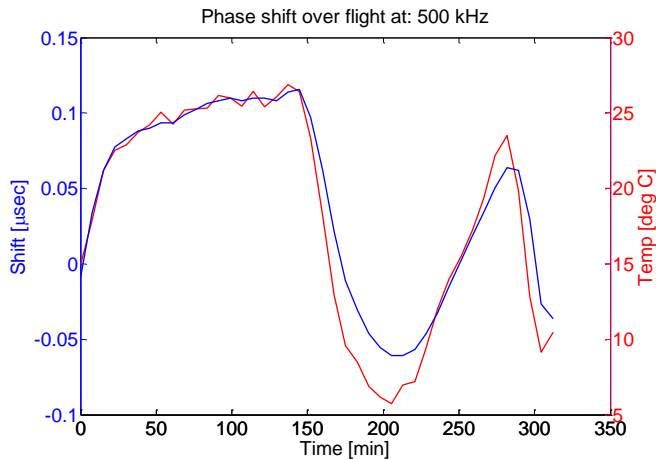


Figure 7 Phase shift and internal temperature for 500kHz wave. Even further matching of data sets

Bolt Condition Monitoring with Temperature Effect

The first goal of this sub-experiment was to transmit a wave pulse from the top plate, into a support pillar, down through the pillar and out into the lower plate where it is picked up by a receiving sensor. This is an example of the “through-transmission” of structural members that is of interest for determining if structural pieces are in their proper place or adequately attached, such as a cover for a component or a properly sealed door. From Figure 8, it is clear that identifying the pulse after passing through the structural member is not a problem. In addition, there is a clear difference (even at various stages of the flight) between the healthy (properly tightened) pillar/bolt and the “damaged” (loosened) pillar. The vertical axes in Figure 8 are at the same limits, the primary difference between the plots is the reduction in amplitude for the damaged scenario. With a looser interface connecting the plates, the energy has a more difficult time passing through. This is already a useful result in identifying whether members

are properly placed/secured. However, the value of this experiment is the repeated data runs taken throughout the high altitude balloon flight. Just as we analyzed deviations in waveforms from the initial ground baseline in the wave speed section, the same treatment will be given to these bolt waveforms.

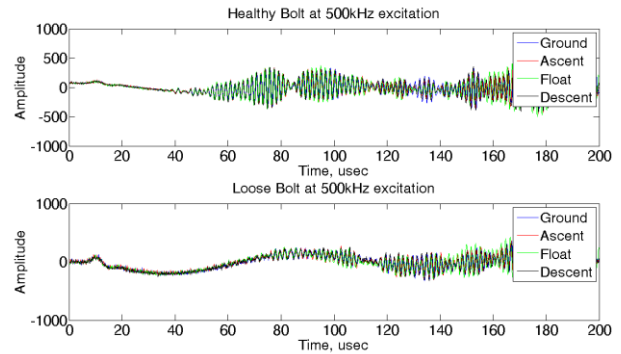


Figure 8 (Top) Healthy bolt path plotted at various stages of flight (Bottom) Loose bolt path at various flight stages

Because of the distance and conversion of the guided wave through plate to rod and rod to plate interfaces, the received waveforms are distorted and have a worse signal-to-noise ratio than other records. Rather than using the phase shift method which is problematic in this data, the records were simply subtracted from one another. The total deviation of the full record will give insight into how far the wave has shifted from the baseline. The absolute value of the difference is taken for every dataset; therefore the magnitude of the deviation is represented in the following plots. Starting with Figure 9, the difference seen throughout the flight is most apparent when the temperature drops to its lowest. However, at this 100kHz excitation, the trend isn’t strong. As the excitation frequency increases the deviations do more strongly follow the temperature changes. In Figure 10, the 300kHz excitation deviations are larger in magnitude and more strongly follow the temperature profile. And in Figure 11, the deviation is greatest and most distinct, particularly when the temperature hits its lowest which is also when the temperature has deviated greatest. Once again, the link between waveform changes and temperatures seems to be strong.

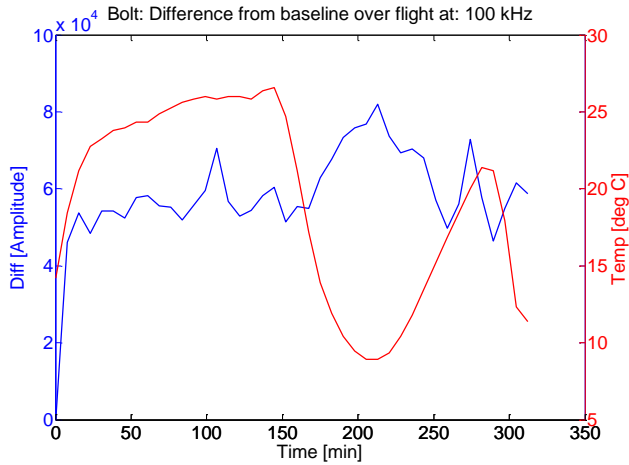


Figure 9 Deviation of waveform during flight from initial ground level baseline at 100kHz

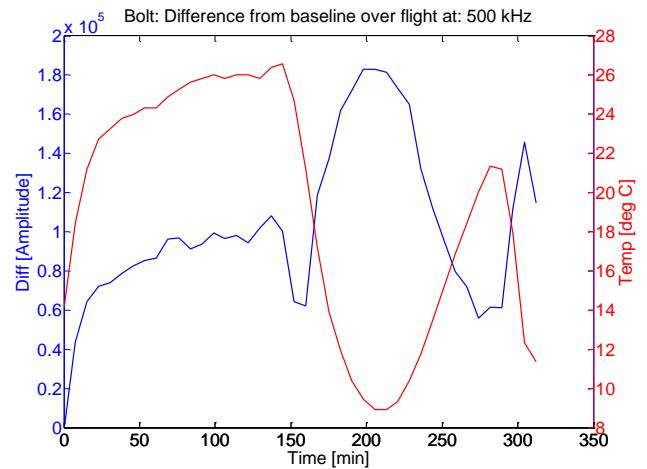


Figure 11 Deviation of waveform during flight from initial ground level baseline at 500kHz

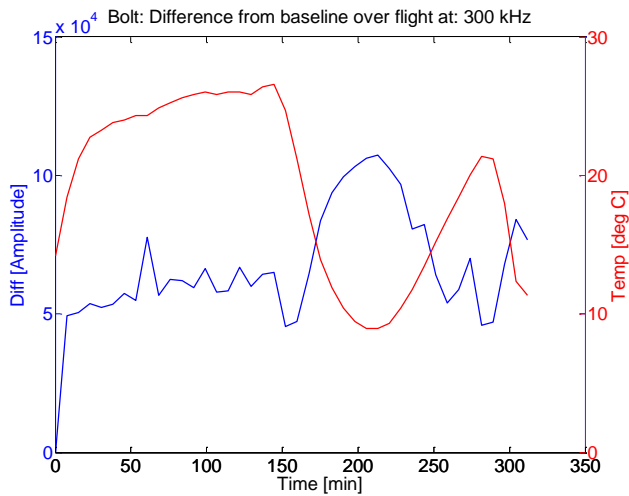


Figure 10 Deviation of waveform during flight from initial ground level baseline at 300kHz

As a final note for the moment on the bolt condition monitoring, zooming in on Figure 8 reveals an interesting characteristic of the waveforms during flight. Figure 12 is a zoomed in view at the 500 kHz excitation. In the loose bolt and a little in the healthy bolt, the amplitude right at the start of float is larger than any of the others. This is possible due to the manner in which the plates and rods are contracting in the colder temperatures. The plates and rods are of dissimilar materials and will contract at different rates. Therefore, a possibility is that the rod is contracting around the plate and bolts, possibly tightening the bolt connection allowing greater energy transmission of the wave pulse and consequently a higher amplitude recorded for the coldest portion of the flight. This has consequences not only for monitoring bolt conditions, but in understanding the thermal cycling on bolts for aircraft and satellites.

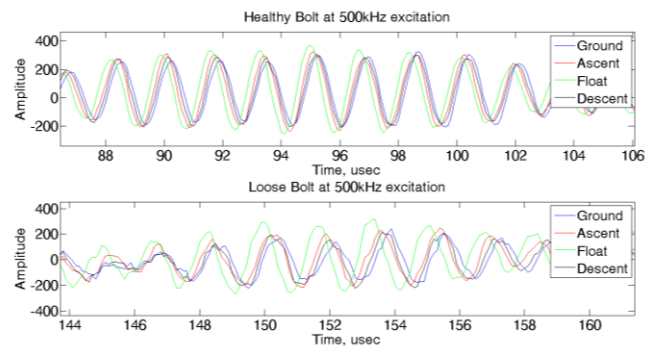


Figure 12 Zoomed in view of the loose and tight bolts showing an increased amplitude right at the start of float

Crack Detection

Two main methods were considered when laying out sensors to collect data for the crack detection at varying altitudes: transmission through the crack and reflection off of the crack. Figure 13 plots each of these sensors at various stages of the flight. First, let's double check that the methods we planned on using make sense given the data. The top plot is the free path and the bottom plot is the crack-obstructed path. Considering through transmission, the bottom plot has a reduced amplitude (plots are the same scale) which would be expected as the crack scatters and prevents some energy from reaching the sensor directly. The second method, the top plot shows the reflection off the crack at about 80 microseconds. The next step is to determine whether the data collection through the duration of the flight had any effect on the ability to detect a crack such as this.

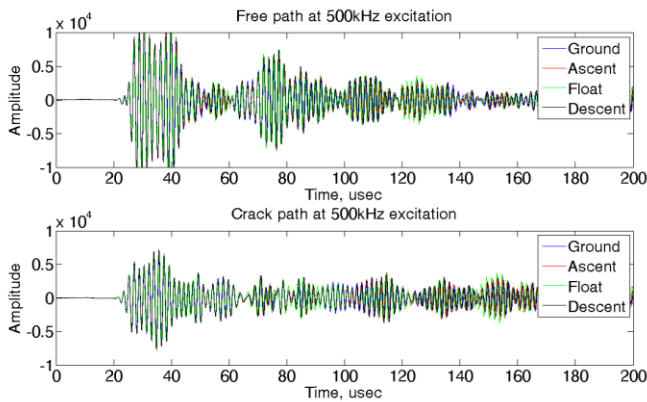


Figure 13 (Top) Unobstructed sensor path to collect reflection coming directly back from crack (Bottom) Sensor waveform with crack obstructing path (transmission)

The same approach will be used on this dataset as was used for the bolt monitoring. The records throughout the flight will be subtracted from the baseline ground set and deviations in the response will be inspected. Figure 14 through Figure 16 illustrate the trends of the deviations from ground baseline. It is a familiar pattern at this point where the deviations follow the temperature. Greater temperature deviations from startup temp lead to greater waveform deviations and higher frequency give larger deviations. The trend in the crack detection data really only follows the wave speed phase shift trend from earlier and no extra notable differences are observed. The simulated crack used is a machined slot and is therefore a large gap. If the crack were thinner the contraction and expansion of the material may have had more interesting results as the material tried push and pull on itself around the crack. For now, this portion of the experiment serves to enhance the data collected for the wavespeed phase shift analysis.

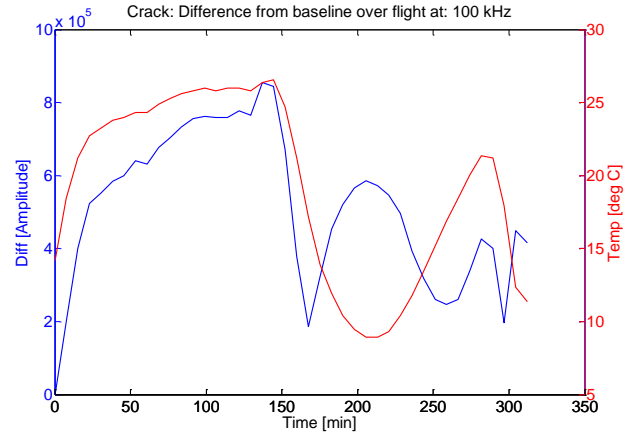


Figure 14 Magnitude difference for through transmission crack path at 100kHz

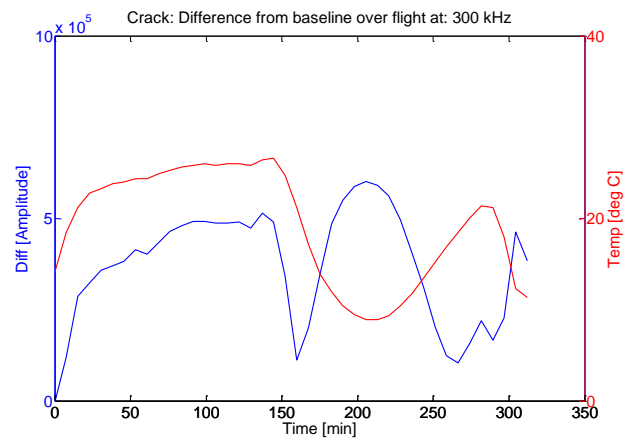


Figure 15 Magnitude difference for crack path at 300kHz

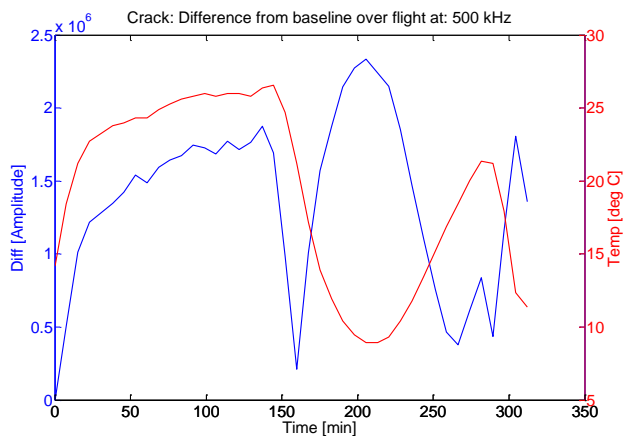


Figure 16 Magnitude difference for crack path at 500kHz

CONCLUSIONS

This paper presented results from a high altitude balloon flight whose payload contained several experiments focused on

advancing the understanding of SHM for space applications. The data presented here focused on the active SHM experiments which used piezoelectric sensors to generate and receive elastic waves in the 50 to 500kHz range. The active SHM experiment focused on three things; looking at changes in wavespeed throughout the flight by observing phase shifts from a ground baseline state, checking on the ability to transmit an elastic wave pulse through a bolted structural member and checking on condition monitoring of tight and loose bolts throughout the flight, and evaluating detection and condition monitoring of a crack. It was found that all experimental goals were heavily influenced by temperature changes. Through use of analytical methods relating guided wave propagation and temperature and further laboratory tests, the effect of temperature will later be subtracted out and any remaining deviation in the flight data can be explored and attributed to environmental factors such as pressure drop.

ACKNOWLEDGEMENT

The flight opportunity was provided by the NASA Flight Opportunities Program. The Federal Aviation Administration (FAA) through the Center of Excellence for Commercial Space Transportation and NMT Department of Mechanical Engineering as well as the Air Force Research Laboratory provided financial support for the payload and flight integration. In addition, thanks should be given to Metis Design Corporation and Seth Kessler for the use of the SHM hardware and insight in the use and interpretation of the system.

REFERENCES

- [1] Reiser, W., Runnels, B., White, C., Light-Marquez, A., Zagrai, A., Siler, D., Marinsek, S., Murray, A., Taylor, S., Park, G., Farrar, C., Sansom, R., 2012, "Design, Development, and Assembly of Sub-orbital Space Flight Structural Health Monitoring Experiment", *Health Monitoring of Structural and Biological Systems 2012*. Proceedings of the SPIE Vol. 8348
- [2] Siler, D., Cooper, B., White, C., Marinsek, S., Zagrai, A., MacGillivray, J., Gutierrez, J., Tena, K., Magnuson, L., Puckett L., Klepper, J., Jorgensen, A., Kessler, S., 2012, "Design, Development, and Assembly of Space Flight Structural Health Monitoring Experiment", *Proceedings of the ASME 2012 Conference on Smart Materials, Adaptive Structures and Intelligent System*. September 19-21, 2012, Stone Mountain, Georgia.
- [3] Arritt, B.J., Robertson, L.M., Henderson, B.K., Ouyang, L., Beard, S., Clayton, E., Todd, M.D., Doyle, D., Zagrai, A., Buckley, B.J., Ganley, J.M., Welsh, J.S., 2008, "Structural Health Monitoring; an Enabler for Responsive Satellites", *49th AIAA/ASME/ASCE/AHS/ASC Structures, Structural Dynamics, and Materials Conference*. April 7-10, Schaumburg, IL.

[4] Dodson, J.C., Inman, D.J., 2013, "Thermal Sensitivity of Lamb Waves for Structural Health Monitoring Applications", *Ultrasonics* **53** pp. 677-685.

[5] Croxford, A.J., Moll, J., Wilcox, P.D., Michaels, J.E., 2010, "Efficient Temperature Compensation Strategies for Guided Wave Structural Health Monitoring", *Ultrasonics* **50** pp. 517-528.

[6] Konstantinidis, G., Wilcox, P.D., Drinkwater, B.W., 2007, "An Investigation Into the Temperature Stability of a Guided Wave Structural Health Monitoring System Using Permanently Attached Sensors", *IEEE Sensors Journal* **7** (5) pp. 905-912.

[7] "Payload User's Guide – SBS", 2011, Near Space Corporation. pp 10. Revision A.